Planetary and Space Science 113-114 (2015) 336–346

Contents lists available at ScienceDirect

Planetary and Space Science

journal homepage: www.elsevier.com/locate/pss

Upper atmosphere temperature structure at the Venusian terminators: A comparison of SOIR and VTGCM results

S.W. Bougher [a,*], A.S. Brecht [b,c], R. Schulte [d], J. Fischer [e], C.D. Parkinson [a], A. Mahieux [f,g], V. Wilquet [f], A. Vandaele [f]

[a] Department of Atmospheric, Oceanic, and Space Sciences, University of Michigan, Space Research Building, 2455 Hayward St., Ann Arbor, MI 48109, USA
[b] Bay Area Environmental Research Institute, Sonoma, CA 95476, USA
[c] NASA Ames Research Center, MSC 245-3, Moffett Field, CA 94035, USA
[d] Santa Clara University, 500 El Camino Real, Santa Clara, CA 95053, USA
[e] University of Pennsylvania, Philadelphia, PA 19104, USA
[f] Planetary Aeronomy, Belgian Institute for Space Aeronomy, Brussels, Belgium
[g] Fonds National de la Recherche Scientifique, rue d'Egmont 5, B-1000 Brussels, Belgium

ARTICLE INFO

Article history:
Received 27 February 2014
Received in revised form
30 September 2014
Accepted 20 January 2015
Available online 7 February 2015

Keywords:
Venus
Venus Express mission
Upper atmosphere
Thermal structure
VTGCM
Thermal balance

ABSTRACT

Venus Express SOIR terminator profiles of CO_2 densities and corresponding temperatures have been determined for 132 selected orbits obtained between 2006 and 2013. These recently recalibrated measurements provide temperature profiles at the Venusian terminator over approximately 70–160 km, revealing a striking permanent temperature minimum (at about 125 km) and a weaker temperature maximum (over 100–110 km). In addition, topside temperatures (above 140 km) reveal a warming trend consistent with a typical thermospheric structure. These features are reflected in the corresponding CO_2 density profiles, and provide detailed constraints for global circulation models of the upper atmosphere.

New Venus Thermospheric General Circulation Model (VTGCM) simulations are presented for conditions appropriate to these SOIR measurements. In particular, solar minimum to moderate fluxes are specified and mean values of eddy diffusion and wave drag parameters are utilized. Recent upgrades to the VTGCM code now include more realistic lower boundary conditions at ~70 km near cloud tops. Model temperature profiles are extracted from the terminators that correspond to five latitude bins presently used in the SOIR data analysis. Averaging of VTGCM temperature profiles in each of these bins (at each terminator) is conducted to match SOIR sampling. Comparisons of these SOIR and VTGCM temperature profiles are shown. Most notably, the observed temperature minimum near 125 km and the weaker temperature maximum over 100–110 km are generally reproduced by the VTGCM at the correct pressure/altitude levels. However, magnitudes of simulated and measured temperatures are somewhat different as a function of latitude. In addition, VTGCM evening terminator (ET) temperatures are simulated to be modestly warmer than corresponding morning terminator (MT) values, a result of stronger ET than MT zonal winds at/above about 130 km. The SOIR terminator temperatures thus far do not reveal this consistent trend, suggesting the VTGCM climate based winds may not precisely represent the averaged conditions during SOIR sampling. Overall, these data-model comparisons reveal that both radiative and dynamical processes are responsible for maintaining averaged temperatures and driving significant variations in terminator temperature profiles.

1. Introduction and motivation

From past observations it has been noted that Venus's upper atmosphere has two dominating circulation patterns (Bougher et al., 1997, 2006; Schubert et al., 2007). One pattern occurs in the region between the surface and the top of the cloud deck (~70 km). This region is dominated by a stable wind pattern flowing in the direction of the planet spin and is faster than the Venus rotation. This flow is known as a retrograde superrotating zonal flow (RSZ). The second pattern occurs above ~120 km and has been inferred (from various observations) to be a relatively stable mean subsolar-to-antisolar flow (SS–AS). Venus has spatially variable heating in the upper atmosphere by solar radiation (EUV, UV, IR), thus providing huge day–night temperature and corresponding pressure gradients which generate the dominant SS–AS flow pattern. In the altitude range of 70–120 km (i.e. the transition region), the two major flow patterns are

* Corresponding author. Tel.: +1 7346473585.
E-mail address: bougher@umich.edu (S.W. Bougher).

http://dx.doi.org/10.1016/j.pss.2015.01.012
0032-0633/

superimposed, often with large variations on short timescales. Ground-based measurements have been largely used to monitor these time variable winds above the cloud tops (Clancy and Muhleman, 1991; Lellouch et al., 1997; Schubert et al., 2007; Clancy et al., 2008). This interaction typically produces at least three modifications to the general flow: (a) a shift in the divergence of the flow from the subsolar point toward the evening terminator, (b) stronger evening terminator winds than those along the morning terminator, and (c) a shift in the convergence of the flow away from midnight and toward the morning terminator. These wind variations also have implications for the underlying temperature structure about the planet.

The investigation of these flow patterns has been achieved (thus far) in concert with the examination of temperature, density and nightglow distributions (horizontal) that have provided proxy estimates of the corresponding wind components, and their variations, as a function of altitude and time. Ongoing measurements, both spacecraft and ground-based, are being made in the effort to construct a realistic climatology of the atmospheric temperature structure. However, departures from this 2-component wind model (residuals) are becoming more apparent, as these ground-based and recent spacecraft measurements confirm significant atmospheric variability (both temporal and spatial) that cannot be easily explained. This new paradigm suggests new sources of dynamical variability, including gravity wave and planetary wave forcing mechanisms. For this paper, we focus upon the upper atmosphere temperature structure (and its spatial and temporal variations) that must be closely connected to these winds fields.

Detailed observations of the Venus atmospheric temperature structure began with the Pioneer Venus (PV) mission in 1978. The Pioneer Venus Orbiter (PVO) provided information about the region from ~70 km in altitude (cloud tops) to ~100 km using both infrared radiometry (Taylor et al., 1980) and radio occultations (Kliore and Patel, 1980). Extensive temperature data was also collected above 140 km, using the PV Orbiter Neutral Mass Spectrometer (Niemann et al., 1979, 1980) as well as by monitoring the decay of the orbiter's orbit due to atmospheric drag (Keating et al., 1980). The PV mission also consisted of four small probes which collected in situ measurements of temperature at selected latitudes and local times (LT) as the probes descended through the atmosphere (Seiff and Kirk, 1982).

These PV measurements, along with previous measurements from the Venera and Mariner missions, were used to construct two empirical models of the upper atmosphere above 100 km, VTS3 (Hedin et al., 1983) and the Venus International Reference Atmosphere, or VIRA (Keating et al., 1985). These models give global temperature profiles of the atmosphere and are used widely by the Venus science community. However, they have their limitations (Soret et al., 2012; Brecht and Bougher, 2012). As mentioned above, the most comprehensive PV measurements occurred below 100 km and above 140 km, leaving a gap where the empirical models perform poorly.

New measurements of the thermal structure of the Venusian atmosphere offer the opportunity to improve these empirical models. Among these are measurements being made by various instruments on the Venus Express (VEx) spacecraft, which was launched in 2005 and entered orbit in 2006. The Venus Express Radio Science experiment (VeRa) uses radio occultation measurements to provide temperature data stretching roughly from 40 to near 90 km in altitude (Tellmann et al., 2009, 2012). The VIRTIS (Visible and Infrared Thermal Imaging Spectrometer) instrument provides coverage on the nightside of Venus up to about the same altitude (Grassi et al., 2010; Lee et al., 2012; Migliorini et al., 2012), and the dayside over 100–150 km. The SPICAV (Spectroscopy for Investigation of Characteristics of the Atmosphere of Venus) instrument also focuses on the nightside and provides data from ~90 km to ~140 km (Bertaux et al., 2007; Piccialli et al., 2013).

Finally, SOIR (Solar Occultation at Infrared) offers an innovative way to study the temperature structure of the atmosphere and is the focus of this study. SOIR makes observations solely at the morning and evening terminators (LT=6:00 and LT=18:00, respectively); these are local times (LT) of great interest because of the dramatic changes that occur across them. Spanning ~70 km to ~160 km, the SOIR measurements are also valuable because they cover the gap from 100 km to 140 km where prior observations were sparse. In addition, SOIR temperature measurements span the transition region (defined above), which is characterized by highly variable wind flow patterns. Corresponding variations in the temperature structure are expected as well. In the sections that follow, SOIR mean temperature profiles for five separate latitude bins are presented and compared to modeled profiles simulated by the Venus Thermosphere General Circulation Model (VTGCM). These SOIR profiles are described in detail in a companion paper of this special issue (Mahieux et al., 2015).

2. The SOIR dataset

The SOIR Instrument has been thoroughly described in the literature (Nevejans et al., 2006; Mahieux et al., 2008, 2009, 2010; Vandaele et al., 2013), for brevity this section is only a summary of the instrument and the technique used to obtain information about the temperature of the Venusian atmosphere at the terminators. SOIR is one of the three channels on the SPICAV instrument and is used to observe the Sun through the atmosphere of Venus. That is, the line of sight of the channel is towards the sun and as Venus Express moves along its orbit, the line of sight passes through the Venusian atmosphere at successive tangent altitudes. The SOIR measurements are scientifically meaningful as they range from about 70 km to around 160 km. The lower boundary is marked by the total absorption by clouds and the upper limit is the point where the strongest CO_2 band in the SOIR wave number range can be detected (Mahieux et al., 2012).

The SOIR instrument operates in the infrared at wavelengths between 2.2 and 4.3 μm and has a spectral resolution varying between 0.11 and 0.21 cm^{-1}. The system consists of an Echelle grating spectrometer working in the infrared, combined with a TeO_2 Acousto-Optic Tunable Filter (AOTF) for the selection of the diffraction grating orders, of which there are 94. During a typical occultation, four different diffraction orders are scanned quasi-simultaneously (Mahieux et al., 2012). Different orders are able to probe different target molecules during an occultation. For the purposes of constructing temperature profiles, carbon dioxide is the target molecule.

The retrieval of temperature profiles is accomplished using the ASIMAT algorithm, described in Mahieux et al. (2010, 2012, 2015). The atmosphere of Venus is divided into layers which are considered to be spherically homogeneous (the “onion-peeling approximation”). The Optimal Estimation procedure developed by Rodgers (2000) is used to create a CO_2 vertical density profile by inverting the observed SOIR atmospheric transmittance spectra data from a given occultation. A temperature profile is then calculated in an iterative process using the hydrostatic law and the CO_2 volume mixing ratios (VMR). It is assumed that the CO_2 VMR is equal to 96.5% from the surface to 88 km, decreasing to 96% at 100 km, and then connecting to the Keating model CO_2 VMR at 104 km (Keating et al., 1985).

SOIR dataset calibration issues have been addressed in detail in Vandaele et al. (2013). These include changes in the wavenumber calibration procedure of the spectra, the instrument resolution calculation, and the signal-to-noise ratio. This reference also gives a short description of the available European Space Agency (ESA) Planetary Science Archive (PSA) online database. More recently, a slit discretization improvement has been incorporated and is discussed in detail in Mahieux et al. (2015). Briefly, this slit correction is applied as a

function of latitude. Since the vertical resolution of the instrument is varying greatly with the latitude of the measurement, a bias was previously introduced into the retrieval. This was manifested in the results as an altitude shift with latitude. To solve this issue, a multi-ray tracing calculation has been introduced in the inversion procedure. In the improved algorithm, 24 light paths spread on the slit in both directions are now considered, and the measurement at one altitude level is calculated as the algebraic average of the contributions of each path. This improvement slightly modifies the density profiles, and the shape of the profiles (succession of minima and maxima of temperature) is not changed. However, the altitudes at which those minima and maxima occur are shifted to lower altitudes. This effect is more pronounced for Southern observations; i.e. the measurements taken at latitudes lower than 60°N are the most affected, because the vertical resolution step becomes larger than the vertical sampling. As a result, the Northern–Southern asymmetry that was observed in the Mahieux et al. (2012) version has now disappeared. This main algorithm improvement is outlined in detail in Mahieux et al. (2015).

The SOIR dataset utilized in this study consists of temperature profiles from 132 separate solar occultation events between 2006 and 2013 (Mahieux et al., 2015). There are 64 morning terminator (MT) observations and 68 evening terminator (ET) observations. Note that many of the individual profiles span only a part of the altitude range being considered in this study. The observations at each terminator have been grouped into five separate latitude bins (see Table 1). Symmetry about the equator has been assumed in part because of the limited sampling in any given latitude bin regardless of the hemisphere. The dataset is most heavily concentrated in the polar region because of the nature of the Venus Express spacecraft's orbit (Mahieux et al., 2012). Due to the lack of data at lower latitudes, those bins span a larger latitude range. Within each latitude bin, the profiles from each individual orbit have been averaged together to give a mean temperature profile for both the morning and evening terminators. The profiles do not include data points that result from"averaging" temperature data from only a single solar occultation. The mean temperature profiles extend from an altitude of approximately 70–90 km to about 160 km, depending on the latitude bin and terminator being considered, and the orders scanned during the occultations.

Finally, vertical smoothing has been performed on the initial SOIR CO_2 profiles, resulting in smoothed temperature profiles. These 132 improved VAST (Venus Atmosphere from SOIR measurements at the Terminator) temperature profiles are composed of the corresponding 122 profiles described in detail in Mahieux et al. (2015), plus 10 additional profiles that we have included, for which the instrument slit was almost vertical in the atmosphere. The CO_2 density profiles from each spectral set are combined into one single profile defined on a 1 km scale using a moving average algorithm. This moving average performs a weighted linear fit of all available individual density values corresponding to altitudes located within a plus or minus two scale height region. Thereafter, a smoothed temperature profile is derived from this CO_2 density profile using the hydrostatic equilibrium equation.

3. Introduction to the VTGCM

The Venus Thermosphere General Circulation Model (VTGCM) is a 3-D finite difference hydrodynamic model of Venus' upper atmosphere (e.g. Bougher et al., 1988) which is based on the National Center for Atmospheric Research terrestrial Thermospheric General Circulation Model (TGCM). The VTGCM has been thoroughly documented as it has been revised and improved over the last two decades; presented in this section is an overview of the model as implemented recently in the revised version of Brecht (2011), Brecht et al. (2011), and Brecht and Bougher (2012).

Table 1
Shows the number of orbits used to construct the temperature profiles for each latitude bin at both the morning (LT=06) and evening (LT=18) terminators.

Latitude (min)	Latitude (max)	Number of orbits (LT=06)	Number of orbits (LT=18)
0	30	16	11
30	60	7	12
60	70	6	5
70	80	9	7
80	90	26	33

The VTGCM solves the time-dependent primitive equations for the neutral upper atmosphere. The diagnostic equations (hydrostatic and continuity) provide geopotential and vertical motion fields. Additionally, the prognostic equations (thermodynamic, eastward and northward momentum, composition) are typically solved for steady-state solutions for the temperature, zonal and meridional velocity, and the mass mixing ratios of specific species. The VTGCM model domain covers a 5° by 5° latitude–longitude grid, with 69 evenly spaced log-pressure levels in the vertical, extending from ~70 to 300 km (~70 to 200 km) at local noon (midnight). This altitude range ensures that all dynamical influences contributing to the nightglow layers (i.e. NO, O_2, OH) can be captured, and wave propagation above the cloud tops can be addressed. The lower boundary of the VTGCM has recently been improved to include the self-consistent latitude and local time variation of temperatures, zonal and meridional winds, and heights near ~69 km, in accord with current Venus lower atmosphere General Circulation Models and available VIRA datasets (Kliore et al., 1985).

The VTGCM includes parameterizations for CO_2 15-μm cooling, infrared (IR) heating, and extreme ultraviolet (EUV) heating. Reference CO_2 15-μm cooling rates for a given temperature and composition profile are taken from Roldán et al. (2000); cooling rates for the simulated VTGCM temperatures and species abundances are calculated (from these reference rates) based upon a slight modification of the parameterization scheme described previously (e.g. Bougher et al., 1986). The near-IR heating term is incorporated in the VTGCM using an offline simulated look-up table (organized as a function of pressure and SZA), and updated recently using Roldán et al. (2000) rates. The VTGCM can capture the full range of EUV–UV flux conditions. The latest ion-neutral reactions and rates being used in the VTGCM are largely taken from Fox and Sung (2001).

Sub-grid scale wave effects cannot be captured by the VTGCM directly. Instead, wave drag is presently prescribed as Rayleigh friction within the VTGCM in order to mimic the first order wave-drag effects on the mean flow (Bougher et al., 1999; Brecht, 2011). Detailed gravity wave momentum deposition schemes are being tested for replacement of Rayleigh friction within the VTGCM code (Zalucha et al., 2013). However, such schemes are not presently validated for dedicated usage in VTGCM simulations. The eddy diffusion coefficient is prescribed in the form $K = A/\sqrt{n}$ with units of $cm^2\ s^{-1}$ where n is the total number density and A is a constant (see von Zahn et al., 1979). Nightside eddy diffusion has a prescribed maximum value of $1.0 \times 10^7\ cm^2\ s^{-1}$ (see Brecht, 2011).

Several VTGCM model runs were made in order to provide temperature profiles for comparison with the SOIR profiles. Model temperature profiles were extracted at each terminator and profiles from the same latitude bin (0–30°N, 30–60°N, 60–70°N, 70–80°N, 80–90°N) were averaged together to create mean temperature profiles corresponding to the five latitude bins currently used in the SOIR analysis. In the base case, minimum solar fluxes (F10.7=70) were specified as many of the early SOIR measurements were obtained during a period when solar fluxes were small. Mean values of the eddy diffusion and wave drag

parameters were used. Runs were also made with moderate solar fluxes (F10.7 = 130) (corresponding to the weak solar maximum conditions appropriate for the later SOIR observations in 2013) and with minimum and maximum drag parameters in order to explore what effects these parameters would have on the temperature profiles. A summary of the different runs is provided in Table 2.

It is noteworthy that the VTGCM has largely been run as a climate model thus far. This means that model adjustable parameters have been specified to enable time and spatially averaged VEx nightglow distributions (Brecht, 2011), VEx atomic O density distributions (Brecht et al., 2012), and VEx plus ground-based dayside temperatures (for mean conditions) (Brecht and Bougher, 2012) to be reproduced. Nevertheless, the changing SS–AS and RSZ wind components of the real atmosphere provide significant variations of these densities, temperatures, and nightglow distributions over time. In particular, the variability of the transition region (~70–120 km) is significant, and will indeed impact measured SOIR temperature profiles. Further modifications to the VTGCM to address this upper atmosphere variability will be discussed in Section 6.

Table 2
Summary of the solar flux and wave drag parameters used for each of the 4 VTGCM runs used in this comparison. (Solar Min : F10.7 = 70, Solar Mod : F10.7 = 130, wave drag mean = 1 $\times 10^{-4}$ s^{-1}, wave drag min = 7 $\times 10^{-5}$ s^{-1}, Wave Drag max = 2 $\times 10^{-4}$ s^{-1}).

Model run	Solar flux	Wave drag
'Solar Min' (base case)	Minimum	Mean
'Solar Mod'	Moderate	Mean
'Max drag'	Minimum	Maximum
'Min drag'	Minimum	Minimum

4. Results: datasets and simulations

4.1. SOIR temperature profiles

Fig. 1 shows the SOIR temperature profiles for each latitude bin at the morning and evening terminators. Regardless of latitude bin or local solar time, several features are observed across all of the temperature profiles (Mahieux et al., 2015). First, all profiles show a profound minimum in temperature near a pressure level of 2.5 $\times 10^{-5}$ mbar (centered at about 123 km), approaching values as low as 90–100 K. In addition, the profiles reveal a less pronounced local maximum in temperature (up to about 225 K) at pressure levels between 10^{-3} and 10^{-2} mbar, and many show another local minimum near 0.1 mbar. These pressure levels correspond to altitudes of about 100–110 and 95 km, respectively. A general warming trend is evident at both the upper and lower limits of both terminators. The topside warming is consistent with what is expected from a dayside thermospheric structure.

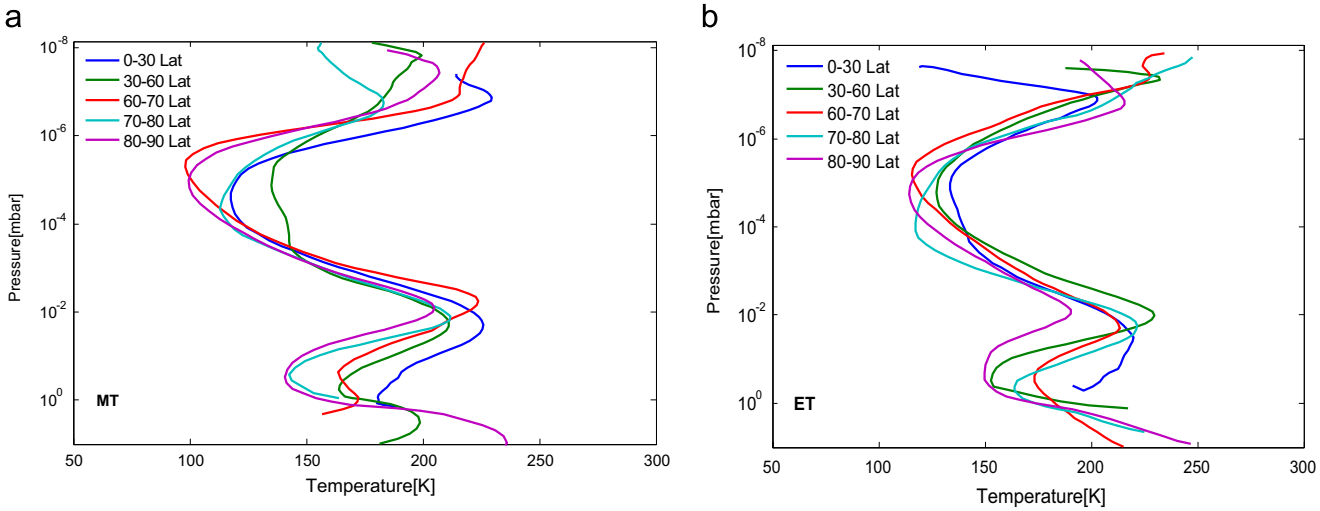

Fig. 1. SOIR mean temperature profiles for each latitude bin at the morning (left) and evening (right) terminators. The vertical axis is given in mbar.

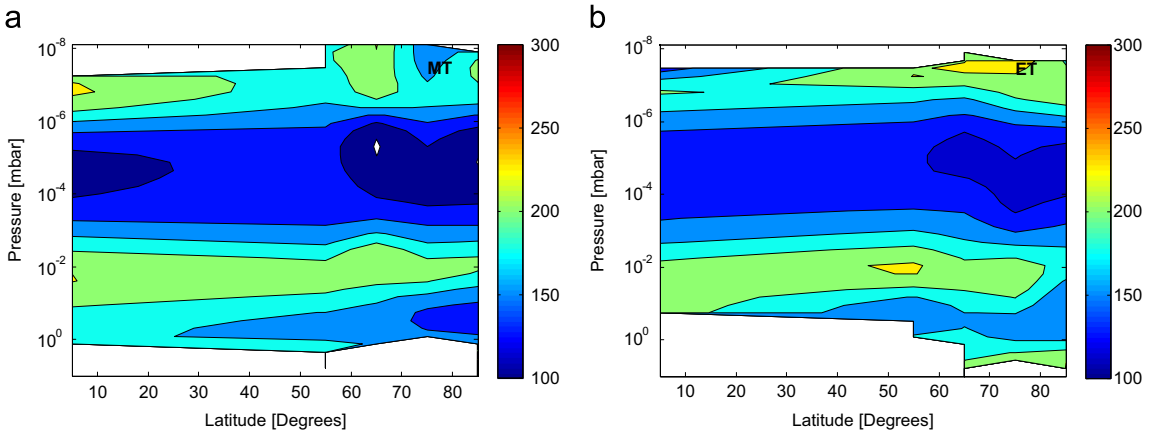

Fig. 2. Two dimensional mean temperature contour plots obtained from 132 individual SOIR orbits, averaged into 5-standard latitude bins. Areas for which no data is available appear white. The vertical axis is given in mbar.

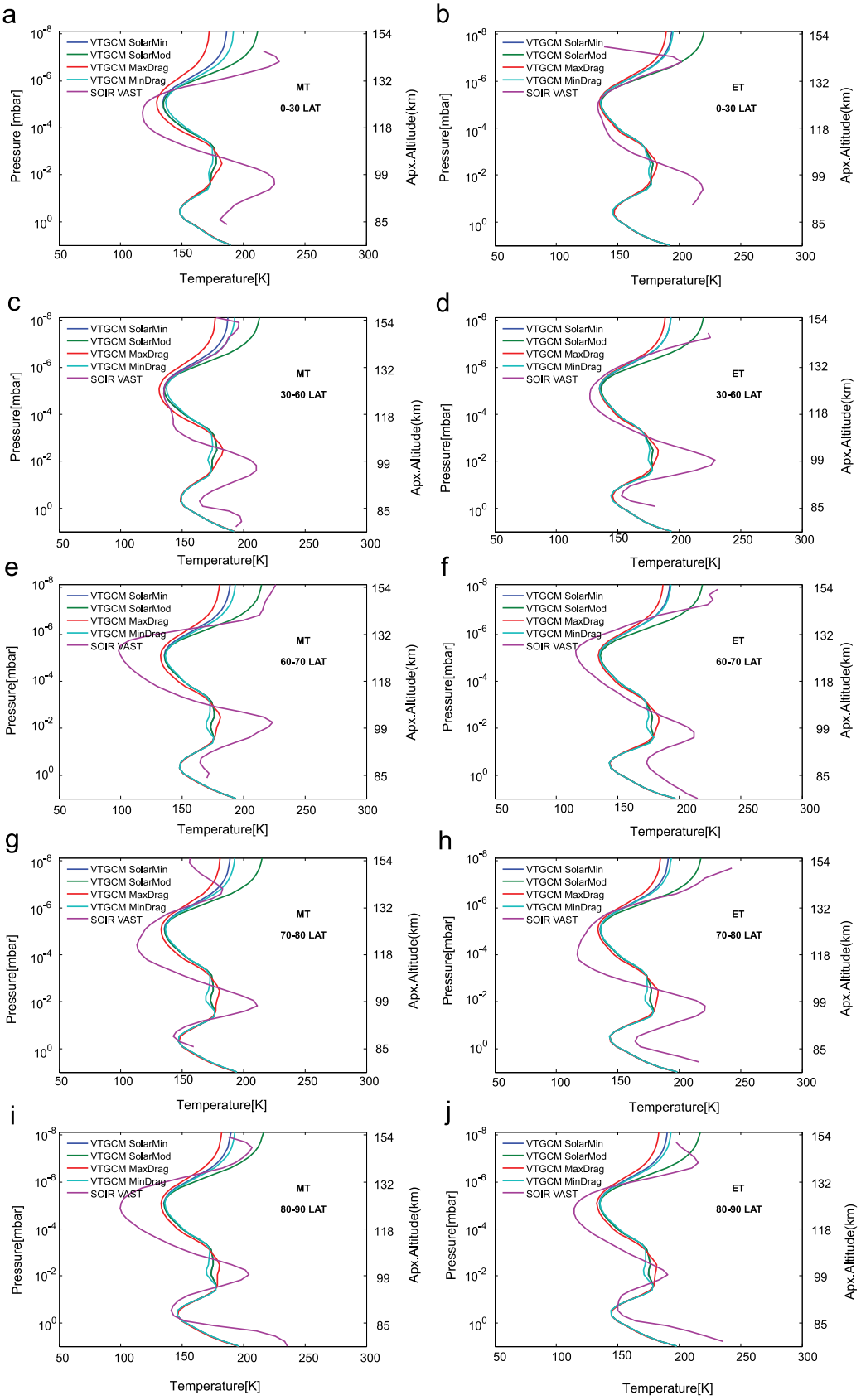

Fig. 3. Plots showing a comparison of the SOIR temperature profiles versus profiles obtained from various model runs of the VTGCM. Morning terminator (left column) and evening terminator (right column) plots are provided for each of the 5-latitude bins (detailed in Table 1). The vertical axis throughout is given in mbar.

However, there are clear discrepancies between the profiles for the different latitude bins. This is shown more clearly in Fig. 2, which shows the mean temperature structure across all latitudes at both terminators. To create these contour maps, the SOIR observations continue to be sorted into the same 5-latitude bins as before. The MT map shows the coldest temperature minima (approaching 90–100 K) at high latitudes (60–90°) and nearest the equator (0–30°), with warmer temperatures at mid-latitudes (~140 K). Conversely, the ET maps illustrate temperatures that cool from the equator (~130–140 K) toward the pole (~120 K). Both maps reveal a warm layer (~100–110 km) that is relatively uniform in temperature (~210–220 K) from the equator to nearly the pole. However, the ET map shows a cold polar region at these altitudes that does not appear at the MT. Finally, topside temperatures in both maps (above ~150 km) show temperatures that vary (±20–30 K) with latitude with a mean value of about 200 K. According to Mahieux et al. (2015), there is good confidence in VAST temperature profiles in the 80–150 km region. However, with only a limited number of orbits available for study thus far, especially in certain latitude bins (over 60–70°), it is difficult to quantify the true extent to which the climate averaged temperature of the Venusian upper atmosphere is truly latitude-dependent. It is noteworthy that the smoothed VAST temperature profiles used in this analysis (instead of averaged raw profiles) provide a latitude map that reduces the latitude variations, more in agreement with VTGCM predictions.

4.2. Comparisons with VTGCM temperature profiles

As mentioned above, the VTGCM uses a log-pressure scale. To facilitate a direct comparison between the VTGCM and SOIR temperature profiles, an interpolation scheme was applied to the SOIR profiles to give temperatures at the exact pressure levels specified by the VTGCM. Fig. 3 shows how the VTGCM profiles are compared to the SOIR profiles for each latitude bin on a millibar pressure scale. The VTGCM simulates the relative shape of the retrieved upper-atmospheric temperature profiles at the Venusian terminators very well. Like the SOIR profiles, the VTGCM profiles all show a consistent temperature minimum near ~125 km and a local temperature maximum near 100–105 km. VTGCM temperatures also show another minimum near 85–90 km, consistent with most of the SOIR profiles poleward of 30° latitude.

However, there are also significant differences between the SOIR and VTGCM temperature profiles. The VTGCM in general shows smaller temperature differences from one altitude to another. For example, at the minimum temperature point around 125 km altitude, matching SOIR and VTGCM temperatures (about 125–130 K) occur at the ET (0–30°) and at both MT and ET (30–60°). However, VTGCM temperatures are as much as 40 K warmer than SOIR values at high latitudes (60–90°) along the MT. In addition, at the local maximum point (100–110 km), the VTGCM predicts temperatures up to 40 K colder than the SOIR profiles (at low latitudes); this discrepancy decreases to 0–20 K at higher latitudes (80–90°). Missing aerosol heating in the VTGCM may be responsible for this temperature difference that varies as a function of latitude (see Section 5). Topside temperatures computed by the VTGCM for solar moderate conditions (220 K) seem to approach some SOIR values; however, solar minimum VTGCM temperatures are at least 20 K colder. It is noteworthy that SOIR temperature retrievals may not be available up to 160 km in all latitude bins for this topside (thermosphere) comparison. When wave drag parameters in the VTGCM were modified (i.e. changing the zonal wind magnitudes), the only significant temperature changes were seen above 140 km. Finally, the VTGCM profiles show almost no latitudinal variation (see Fig. 4), which is consistent with the weak variation of VTGCM temperatures within a given latitude bin. This is in contrast to the latitude variations illustrated (see Fig. 2) and described above based upon the ET and MT maps of VAST temperatures.

4.3. Temporal variation in the VTGCM

The VTGCM profiles exhibit clear and consistent differences between the morning and evening terminators. Most notably, for all latitude bins, the temperatures at high altitudes are warmer at the evening terminator (ET) than they are at the morning terminator (MT). This is a result of stronger net zonal winds at the ET carrying heat from the dayside to the nightside of the planet; i.e. recall that RSZ winds add to the SS–AS flow across the ET while subtracting from the SS–AS flow across the MT, resulting in an asymmetry in the net zonal winds between the terminators. Fig. 5 offers a comparison between the VTGCM mean temperature profiles for the 0–30° latitude bin (the graph is representative of the trend seen in every latitude bin) as well as corresponding heat balance plots. While many of terms do not change very much from the morning to the evening terminator, at high altitudes the advection term is clearly larger in the evening than in the morning, consistent with stronger ET zonal winds and horizontal temperature gradients.

Currently, there is little evidence of a similar (consistent) trend in the SOIR profiles (see Fig. 5). However, there are a couple of complicating factors that might explain why clear differences between the terminators are not evident in the SOIR data. First, only a limited number of individual orbits were able to obtain data for the high altitude range in which the differences are most pronounced in the VTGCM. Second, small “kinks” are evident at the top of many of the SOIR profiles which are unlikely to be physical. Instead, they are probably a result of the fact that in creating the profiles an initial temperature must be assumed for

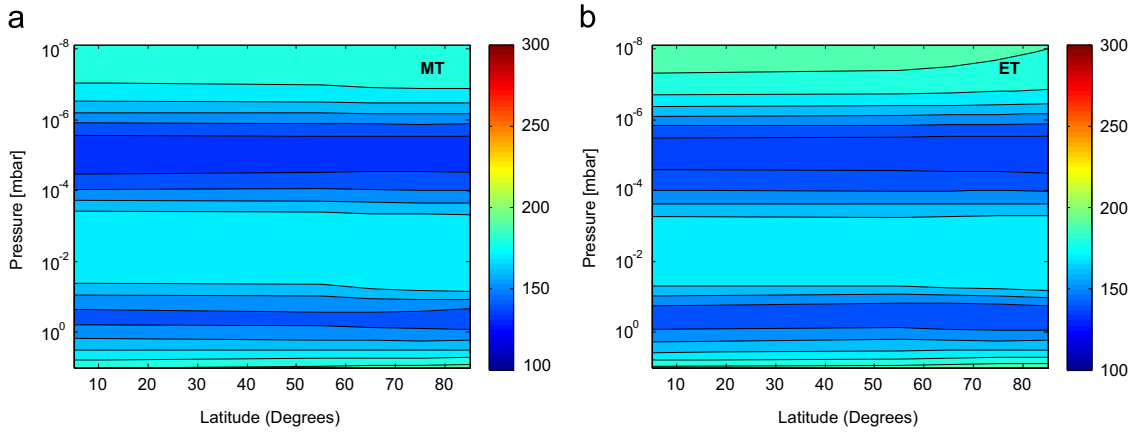

Fig. 4. Two dimensional VTGCM mean temperature contour plots for the morning (left) and evening (right) terminators. The vertical axis is given in mbar.

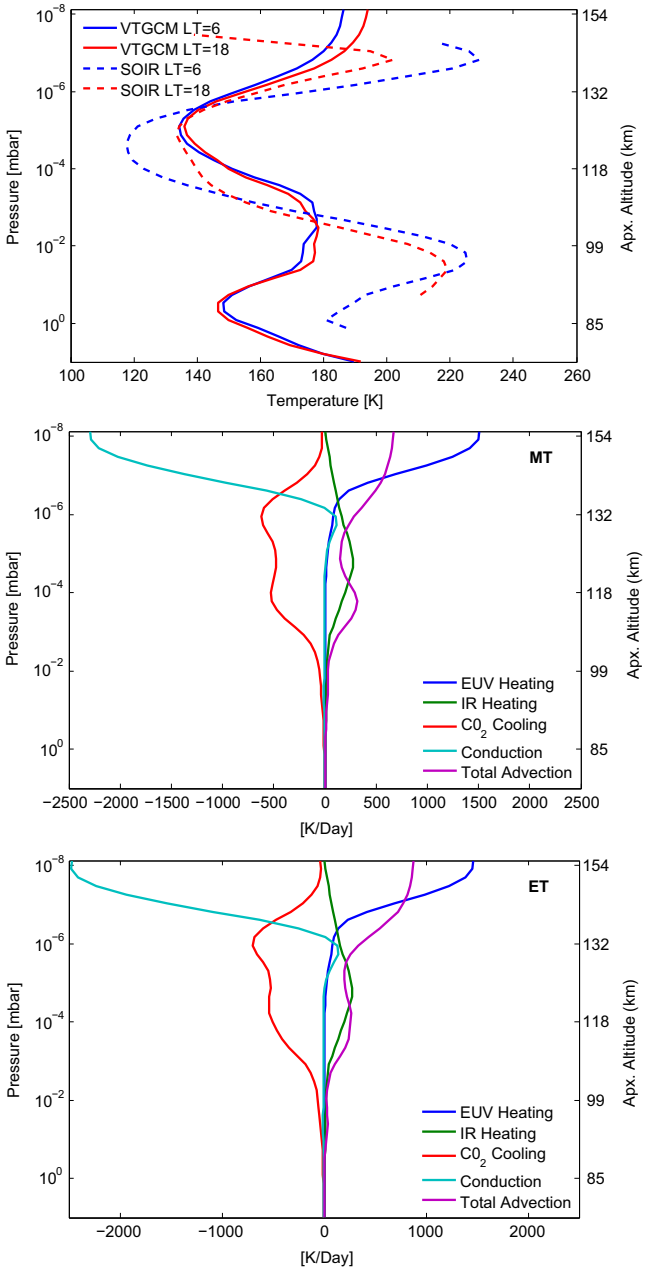

Fig. 5. Top: Morning (blue solid) and evening (red solid) mean VTGCM temperature profiles for the 0–30 latitude bin with dashed lines for SOIR; Middle: Morning terminator VTGCM heat balance outputs at 17.5°N; Bottom: Evening terminator heat balance plot for the same latitude (notice the purple curve is shifted to the right at high altitudes). The vertical axis throughout is given in mbars.

the top of the profile (Mahieux et al., 2015). It takes about one scale height for the profile to become completely independent of the initial condition. Finally, relatively large standard deviations exist among the individual profiles that comprise the bin averaged VAST temperature profiles. This means that atmospheric variability is large, and the SOIR sampling obtained thus far for the VAST dataset may not be adequate (i.e. more measurements are needed, especially at mid-latitudes) to capture climate average conditions for comparison to the VTGCM.

4.4. Comparison to ground based observations

Observations of the Venusian thermosphere from the Earth's surface have been done. This paper focuses only on one technique, heterodyne spectroscopy of CO_2, due to the specific LT and vertical coverage. The heterodyne spectroscopy of CO_2 at mid-infrared wavelengths is a measurement of the non-local thermodynamic equilibrium emission of CO_2 near 10 μm, which occurs at 0.15 Pa (approximately 110 km) (Sonnabend et al., 2010; Lopez-Valverde et al., 2011). Sonnabend et al. (2008) explain the technique and instrument, Cologne Tuneable Heterodyne Infrared Spectrometer (THIS), in more detail. Table 1 from Sonnabend et al. (2010) lists all the data collected during their three observational periods: March 20–22, 2009; April 2–6, 2009; and June 2–6, 2009. Venus was at inferior conjunction (March 27, 2009) after the March observations and before the April observations. The June observation was at maximum western elongation. Included in the table is the time and location of these measurements. THIS observations at the morning or evening terminators are represented in Fig. 6(a, b) and compared to the SOIR and VTGCM averaged values. The SOIR and VTGCM values are the averaged values within a specific latitude bin at 0.15 Pa (1.5 μbar), as discussed in the previous sections. The bars on the SOIR data represent the range of temperatures for that specific bin, while the bars around the Sonnabend et al. (2010) data correspond to either (1) the range for multiple observations at the specific latitude or (2) the retrieval error if there was only one measurement.

The VTGCM results agree favorably with the SOIR averaged data at this pressure, while both seem to fall on the cooler side compared to Sonnabend et al. (2010) data. Specifically, the three datasets are in better agreement for the ET than the MT. The MT variability could be due to other dynamical processes competing with horizontal convection. However, the VTGCM does not accurately produce the latitude variation as shown and discussed previously, while the SOIR temperatures and Sonnabend et al. (2010) data suggest latitude variation at 0.15 Pa. As explained in Sonnabend et al. (2010), these differences could be due to field of view (FOV) and data dependencies (such as altitude information for both datasets).

Alternatively, Fig. 6(c,d) compares SOIR and VTGCM temperatures at 1.0 Pa (10.0 μbar), corresponding to the maximum value of the temperatures observed by SOIR near ~100–105 km. Both ET and MT comparisons are illustrated; latitude symmetry about the equator is again assumed. The latitude variations displayed confirm that VTGCM temperatures are much colder at low-to-mid latitudes, and appear to approach SOIR values near the poles. Once again, some heating mechanism is missing in the VTGCM at/below ~105 km, especially at low-to-mid latitudes. Section 5 discusses potential sources for this heating.

5. Discussion

The VTGCM and SOIR profiles exhibit the same basic structure, all showing distinct temperature minima and maxima near the same pressure and altitude levels in the atmosphere. However, the magnitudes of the modeled and observed temperatures differ in certain areas. VTGCM heat balance terms help us to understand the underlying physical processes responsible for the matching profiles, and what physics may be missing in the VTGCM in areas where simulated and SOIR temperature profiles do not match.

SOIR datasets show a warm layer at/above ~140–150 km for all latitudes, with significant variations with latitude. Overall, temperatures in this layer vary between 170 and 230 K (Mahieux et al., 2015). According to the VTGCM (see Fig. 5), especially at low latitudes, warm temperatures above ~140 km are due to a combination of extreme ultraviolet (EUV) heating and cross terminator heat transport (advection) from the warm dayside thermosphere. There is good correspondence between the VTGCM and SOIR temperatures in this region (see several panels in Fig. 3). Variations about these mean

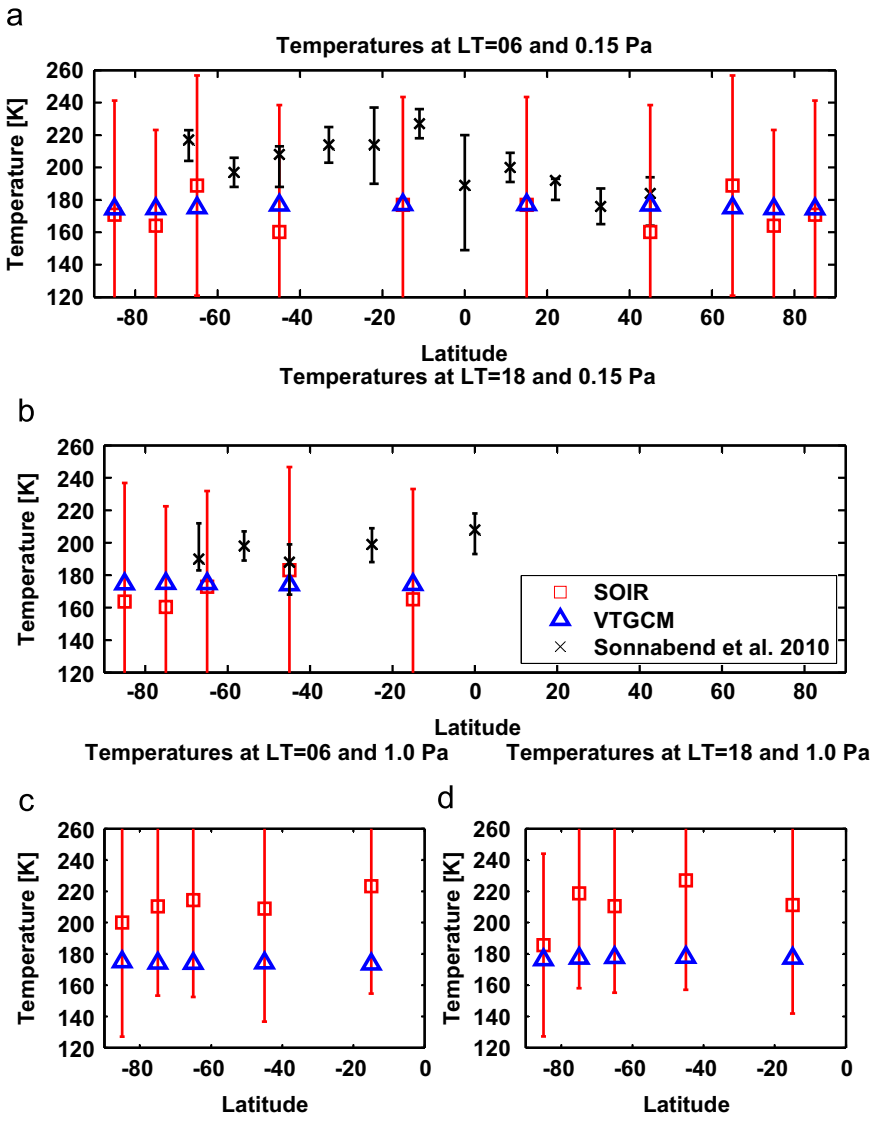

Fig. 6. SOIR (red squares) and VTGCM (blue triangles) values are the averaged values within a specific latitude bin [0–30°, 30–60°, 60–70°, 70–80°, 80–90°] at the (a) morning terminator (0.15 Pa), (b) evening terminator (0.15 Pa), (c) morning terminator (1.0 Pa), and (d) evening terminator (1.0 Pa). The former (a, b) correspond to roughly 110 km; the latter (c, d) correspond to roughly 102 km. The bars on the SOIR data represent the range of temperatures for that specific bin, while the bars around the Sonnabend data (black) correspond to either (1) the range for multiple observations at the specific latitude or (2) the retrieval error if there was only one measurement. Finally, it is assumed that both VTGCM and SOIR displayed temperatures are symmetric about the equator. For Fig. 6a, both Southern and Northern hemisphere VTGCM and SOIR datapoints are displayed (i.e. mirrored about the equator). However, only Southern hemisphere values are displayed for (b)–(d). (For interpretation of the references to color in this figure caption, the reader is referred to the web version of this paper.)

values, observed on both sides of the terminator, are likely due to the large variability of the actual SS-AS and RSZ winds at these altitudes.

Conversely, the cold layer at ~125–130 km is observed at all latitudes, with differences between the morning and evening sides of the terminator (Mahieux et al., 2015). The VTGCM suggests that cold temperatures in this layer are due to weak near-IR heating at these levels (no EUV heating), and relatively weak transport (advection) at all latitudes along the terminators. A reasonable match of VTGCM and SOIR temperatures in this layer is found at 0–60° latitude, where these heat balance terms are most likely to be appropriate to the SOIR mean profiles. At higher latitudes (60–90°), the very cold temperature minima observed may suggest dynamical processes not captured thus far by the VTGCM (Brecht and Bougher, 2012).

At lower altitudes, a warm layer is observed by SOIR at about 100–110 km, with temperatures around 220 K at low latitudes. Temperatures for this layer are relatively uniform at lower latitudes (less than 80°) but reach colder values when approaching the poles (180–200 K) (Mahieux et al., 2015). These terminator temperature maxima, at lower latitudes in the VTGCM simulations, are largely driven by strong near-IR (4.3 μm) heating advected from the dayside (e.g. Roldán et al., 2000; Brecht et al., 2011, 2012; Brecht and Bougher, 2012). This terminator warm layer is connected to the warm dayside region at ~115 km (at noon) from which day-to-night winds advect heat toward the terminators along constant pressure surfaces. These constant pressure surfaces drop in altitude across the terminators, so that these evening and morning terminator layers are about ~5–10 km lower than that at noon. The top half of this terminator layer shows a reasonable match of SOIR and VTGCM temperatures. However, below ~105 km, this warm layer is missing in the VTGCM (i.e. yielding much colder temperatures than SOIR), suggesting that an additional heating mechanism is needed. This discrepancy between SOIR and VTGCM temperatures (below ~105 km) could be the result of static near-IR heating rates (currently taken from Roldán et al., 2000) which do not accurately reflect the real atmosphere at these altitudes, especially at low latitudes. An interactive calculation of near-IR heating rates within the VTGCM may be needed instead.

Alternatively, this discrepancy in temperatures below ~105 km could be an indication of the presence of aerosols near/below 100 km to which SOIR is not sensitive (Mahieux et al., 2015; Wilquet et al., 2012). Observations and radiative transfer models suggest potential heat sources at/above cloud tops, including aerosol heating in the upper haze layer and the unknown UV absorber (e.g. Crisp, 1986; Bullock and Grinspoon, 2001). Currently, aerosol distributions and associated heating are being investigated using the 1-D CARMA (Community Aerosol and Radiation Model for Atmospheres) model to quantify the magnitude of the potential heating as a function of latitude (Turco et al., 1979; Toon et al., 1988, 1989; Parkinson et al., 2015). Sulfuric acid aerosols make up most of the global cloud deck and accompanying hazes that shroud the surface of Venus (Esposito et al., 1983). As a result, the radiation environment and energy budget at the surface and throughout the atmosphere is strongly affected by the vertical extent, size distribution, and mean optical properties of these particles. These aerosols also serve as a reservoir for sulfur and oxygen, and thus play a major part of the global sulfur oxidation cycle (Mills et al., 2007). Furthermore, recent studies (Zhang et al., 2012) have hypothesized that the upper haze layer could provide the source of sulfur oxides above 90 km. Therefore, studying aerosols is a crucial step toward understanding the radiation environment and chemistry on Venus. The ultimate goal here is to incorporate and test a simplified aerosol heating parameterization into the 70–110 km region of the VTGCM.

In addition to aerosol heating, tides and planetary waves could modify the thermal structure in this region. Hoshino et al. (2012), using a general circulation model similar to the VTGCM, demonstrated that the Kelvin wave propagates up to about 130 km and can have a significant impact on the strength of the zonal winds in the upper atmosphere. It is possible that the incorporation of simulated Kelvin waves into the VTGCM will bring the magnitude of the modeled temperatures more in line with the SOIR measurements.

Finally, consistent differences between the morning and evening temperature profiles are obtained in the VTGCM (above 140 km), but are not manifest in the SOIR profiles. Continuing observations of the Venusian atmosphere by SOIR, as well as improvements to the SOIR temperature retrieval algorithm which are currently underway, offer the possibility of a closer agreement between the climate averaged SOIR and VTGCM mean temperature profiles.

6. Conclusions

A total of 132 individual SOIR temperature profiles covering a wide range of latitudes have been binned together and averaged to give mean upper atmosphere temperature profiles for five latitude bins at both the morning and evening terminators. These profiles were compared to corresponding (bin averaged) profiles generated by the Venus Thermosphere General Circulation Model (VTGCM). The VTGCM-SOIR comparisons conducted here assume that the climate averaged nature of the current VTGCM simulations is an appropriate match to the time averaged SOIR profiles. With this limited SOIR sample of 132 profiles, this may not be the case. Furthermore, the SOIR profiles implicitly include atmospheric variability that the current VTGCM code cannot presently accommodate; future implementation of variable lower boundary wave forcing for the VTGCM is planned.

The VTGCM climate simulations successfully reproduce some of the characteristics of the SOIR terminator temperature structure over 80–160 km. For instance, the altitude and pressure levels of the SOIR and VTGCM temperature maxima and minima match reasonably well. However, the magnitudes of the primary temperature minima sometimes match quite well (e.g. ~110–130 km over 0–60° latitude), while the temperature differences are large (up to 40 K) at higher latitudes. SOIR temperatures for the bottom half of the warm layer near 100–110 km are poorly reproduced by the VTGCM at low latitudes, while SOIR and VTGCM temperatures in this region match much better at polar latitudes. The latitudinal variability of the VTGCM simulated temperatures is presently quite weak, while that of the SOIR dataset shows modest variability that requires further confirmation (i.e. with additional measurements especially at mid-latitudes). Overall, current simulations suggest that the VTGCM can be a valuable tool to investigate the thermal balances (both dynamical and radiative) that give rise to the observed thermal structure. However, additional sources for dynamical variability need to be incorporated in the VTGCM, taking the code beyond its climate model capabilities.

Ongoing research utilizing the VTGCM and SOIR temperature profiles first requires that 3-D model improvements be made to better address upper atmosphere variability. New sources of dynamical variability must be included. These sources include gravity wave momentum deposition (Zalucha et al., 2013), which can be important in regulating the magnitude of the SS-AS and RSZ wind components, which in turn impact the global thermal structure above the cloud tops. Validation of existing momentum deposition formulations needs to be completed before their full scale usage within the VTGCM is warranted. In addition, upward propagating thermal tides and planetary waves (presumably launched from the cloud tops) must also be incorporated into the VTGCM structure utilizing its recently upgraded lower boundary condition routines. Recent GCM simulations (Hoshino et al., 2012) suggest that diurnal Kelvin waves may successfully propagate upward to thermospheric altitudes and subsequently drive variability of nightglow emissions and underlying temperature, wind, and density structures. Such variability may be able to explain the changes in the SOIR terminator temperatures profiles (especially as a function of latitude). Each of these improvements will transition the VTGCM code beyond its present climate model capabilities to better address time and spatial variations that the Venus upper atmosphere exhibits. It is noteworthy that trace specifies (e.g. SOx) are currently being incorporated into the VTGCM to help constrain the global wind components in the region above the clouds tops to 110 km. This capability is required for the incorporation of a simplified aerosol heating parameterization into the 70–110 km region of the VTGCM. This additional heating may be sufficient to match SOIR and VTGCM terminator temperatures below ~105 km.

Secondly, SOIR terminator sampling could be expanded to better characterize the climatology of the temperatures over 80–160 km. Presently, the SOIR sampling at mid-latitudes (60–80° latitude) is rather poor. A proper climatology would require much better sampling in order to (a) confirm the latitudinal variations of the upper atmosphere terminator temperatures (80–160 km), (b) expand the number of profiles that extend up to 160 km, so that topside thermospheric temperatures can be better characterized, and (c) confirm the variation of the secondary maximum region (100–110 km) as a function of latitude. If possible, new SOIR sampling will be performed until the end of the VEx mission to increase the number of CO_2 measurements in these latitude regions of the Venus upper atmosphere.

Finally, it would be instructive to combine SOIR, VIRTIS and VeRA temperature profile analysis at the terminators, along with ground-based datasets, in order to understand the temperature variability and the characteristics of its climatology. Studies along these lines, assimilating datasets from various sources, have already begun with the work of the International Space Studies Institute (ISSI) Thermal Structure Working Group in 2013 and 2014.

Acknowledgments

This research was funded by the NASA Venus Express Participating Scientist program through a subcontract from Southwest Research

Institute (SwRI) to the University of Michigan (B99073JD). C.D. Parkinson acknowledges support with funding in part by NASA Grant #NNX11AD81G to the University of Michigan. C.D. Parkinson also wishes to thank the International Space Science Institute (ISSI) for their fruitful support for Venus team research over 2013–2015.

References

Bertaux, J.-L., et al., 2007. A warm layer in Venus' cryosphere and high-altitude measurements of HF, HCl, H_2O and HDO. Nature 450, 646–649. http://dx.doi.org/10.1038/nature05974.

Bougher, S.W., Dickinson, R.E., Ridley, E.C., Roble, R.G., Nagy, A.F., Cravens, T.E., 1986. Venus mesosphere and thermosphere. II—Global circulation, temperature, and density variations. Icarus 68, 284–312. http://dx.doi.org/10.1016/0019-1035(86)90025-4.

Bougher, S.W., Roble, R.G.E., Dickinson, R.E., Ridley, E.C., 1988. Venus mesosphere and thermosphere. III—Three-dimensional general circulation with coupled dynamics and composition. Icarus 73, 545–573. http://dx.doi.org/10.1016/0019-1035(88)90064-4.

Bougher, S.W., Alexander, M.J., Mayr, H.G., 1997. Upper atmosphere dynamics: global circulation and gravity waves. In: Bougher, S.W., Hunten, D.M., Phillips, R.J. (Eds.), Venus II: Geology, Geophysics, Atmosphere, and Solar Wind Environment, pp. 259–291.

Bougher, S.W., Engel, S., Roble, R.G., Foster, B., 1999. Comparative terrestrial planet thermospheres 2. Solar cycle variation of global structure and winds at equinox. J. Geophys. Res. 104, 16591–16611. http://dx.doi.org/10.1029/1998JE001019.

Bougher, S.W., Rafkin, S., Drossart, P., 2006. Dynamics of the Venus upper atmosphere: outstanding problems and new constraints expected from Venus Express. Planet. Space Sci. 54, 1371–1380. http://dx.doi.org/10.1016/j.pss.2006.04.023.

Brecht, A., Bougher, S., Gérard, J.-C., Soret, L., 2012. Atomic oxygen distributions in the Venus thermosphere: comparisons between Venus Express observations and global model simulations. Icarus 217 (2), 759–766. http://dx.doi.org/10.1016/j.icarus.2011.06.033.

Brecht, A.S., 2011. Tracing the Dynamics in Venus' Upper Atmosphere (Ph.D. thesis), University of Michigan.

Brecht, A.S., Bougher, S.W., 2012. Dayside thermal structure of Venus' upper atmosphere characterized by a global model. J. Geophys. Res. (Planets) 117, E08002. http://dx.doi.org/10.1029/2012JE004079.

Brecht, A.S., Bougher, S.W., Gérard, J.-C., Parkinson, C.D., Rafkin, S., Foster, B., 2011. Understanding the variability of nightside temperatures, NO UV and O_2 IR nightglow emissions in the Venus upper atmosphere. J. Geophys. Res. 116, E08004. http://dx.doi.org/10.1029/2010JE003770.

Bullock, M.A., Grinspoon, D.H., 2001. The recent evolution of climate on venus. Icarus 150 (1), 19–37. http://dx.doi.org/10.1006/icar.2000.6570.

Clancy, R.T., Muhleman, D.O., 1991. Long-term (1979–1990) changes in the thermal, dynamical, and compositional structure of the Venus mesosphere as inferred from microwave spectral line observations of ^{12}CO, ^{13}CO, and $C^{18}O$. Icarus 89, 129–146. http://dx.doi.org/10.1016/0019-1035(91)90093-9.

Clancy, R.T., Sandor, B.J., Moriarty-Schieven, G.H., 2008. Venus upper atmospheric CO, temperature, and winds across the afternoon/evening terminator from June 2007 JCMT sub-millimeter line observations. Planet. Space Sci. 56, 1344–1354. http://dx.doi.org/10.1016/j.pss.2008.05.007.

Crisp, D., 1986. Radiative forcing of the venus mesosphere: I. Solar fluxes and heating rates. Icarus 67 (3), 484–514. http://dx.doi.org/10.1016/0019-1035(86)90126-0.

Esposito, L.W., Knollenberg, R.G., Marov, M.Y., Toon, O.B., Turco, R.P., 1983. The Clouds and Hazes of Venus. In: Hunten, D.M., Colin, L., Donahue, T.M., Moroz, V.I. (Eds.), Venus, pp. 484–564.

Fox, J.L., Sung, K.Y., 2001. Solar activity variations of the Venus thermosphere/ionosphere. J. Geophys. Res. 106, 21,305–21,336. http://dx.doi.org/10.1029/2001JA000069.

Grassi, D., Migliorini, A., Montabone, L., Lebonnois, S., Cardesìn-Moinelo, A., Piccioni, G., Drossart, P., Zasova, L.V., 2010. Thermal structure of Venusian nighttime mesosphere as observed by VIRTIS-Venus Express. J. Geophys. Res. 115 (E14), E09,007. http://dx.doi.org/10.1029/2009JE003553.

Hedin, A.E., Niemann, H.B., Kasprzak, W.T., Seiff, A., 1983. Global empirical model of the Venus thermosphere. J. Geophys. Res. 88, 73–83. http://dx.doi.org/10.1029/JA088iA01p00073.

Hoshino, N., Fujiwara, H., Takagi, M., Takahashi, Y., Kasaba, Y., 2012. Characteristics of planetary-scale waves simulated by a new Venusian mesosphere and thermosphere general circulation model. Icarus 217 (2), 818–830. http://dx.doi.org/10.1016/j.icarus.2011.06.039.

Keating, G.M., Nicholson, J.Y., Lake, L.R., 1980. Venus upper atmosphere structure. J. Geophys. Res. 85, 7941–7956. http://dx.doi.org/10.1029/JA085iA13p07941.

Keating, G.M., Bertaux, J.-L., Bougher, S.W., Dickinson, R.E., Cravens, T.E., Hedin, A.E., 1985. Models of Venus neutral upper atmosphere—structure and composition. Adv. Space Res. 5, 117–171. http://dx.doi.org/10.1016/0273-1177(85)90200-5.

Kliore, A.J., Patel, I.R., 1980. Vertical structure of the atmosphere of Venus International Reference Atmosphere from Pioneer Venus orbiter radio occultations. J. Geophys. Res. 85, 7957–7962. http://dx.doi.org/10.1029/JA085iA13p07957.

Kliore, A.J., Moroz, V.I., Keating, G.M., 1985. The Venus International Reference Atmosphere. Adv. Space Res. 5.

Lee, Y.J., Titov, D.V., Tellman, S., Piccialli, A., Ignatiev, N., Pätzold, M., Häusler, B., Piccioni, G., Drossart, P., 2012. Vertical structure of the Venus cloud top from the VERA and VIRTIS observations onboard Venus Express. Icarus 217 (2), 599–609.

Lellouch, E., Clancy, T., Crisp, D., Kliore, A.J., Titov, D., Bougher, S.W., 1997. Monitoring of Mesospheric Structure and Dynamics. In: Bougher, S.W., Hunten, D.M., Phillips, R.J. (Eds.), Venus II: Geology, Geophysics, Atmosphere, and Solar Wind Environment, pp. 295–324.

Lopez-Valverde, M.A., Sonnabend, G., Sornig, M., Kroetz, P., 2011. Modelling the atmospheric CO_2 10-micron non-thermal emission in Mars and Venus at high spectral resolution. Planet. Space Sci. 59, 999–1009. http://dx.doi.org/10.1016/j.pss.2010.11.011.

Mahieux, A., et al., 2008. In-flight performance and calibration of SPICAV SOIR onboard Venus Express. Appl. Opt. 47, 2252–2265. http://dx.doi.org/10.1364/AO.47.002252.

Mahieux, A., Wilquet, V., Drummond, R., Belyaev, D., Fedorova, A., Vandaele, A., 2009. A new method for determining the transfer function of an acousto optical tunable filter. Opt. Express. 17 (3), 2005–2014.

Mahieux, A., Vandaele, A.C., Neefs, E., Robert, S., Wilquet, V., Drummond, R., Federova, A., Bertaux, J.L., 2010. Densities and temperatures in the Venus mesosphere and lower thermosphere retrieved from SOIR on board Venus Express: retrieval technique. J. Geophys. Res. 115 (E14), E12,014. http://dx.doi.org/10.1029/2010JE003589.

Mahieux, A., Vandaele, A.C., Robert, S., Wilquet, V., Drummond, R., Montmessin, F., Bertaux, J.L., 2012. Densities and temperatures in the Venus mesosphere and lower thermosphere retrieved from SOIR on board Venus Express: carbon dioxide measurements at the Venus terminator. J. Geophys. Res. (Planets) 117, E07001. http://dx.doi.org/10.1029/2012JE004058.

Mahieux, A., Vandaele, A.-C., Bougher, S.W., Yelle, R.V., Drummond, R., Robert, S., Wilquet, V., Piccialli, A., Montmessin, F., Tellmann, S., Patzold, M., Hausler, B., Bertaux, J.-L., 2015. Update of the Venus density and temperature profiles at high altitude measured by SOIR on board Venus Express. Planet. Space Sci. 113-114, 310–321.

Migliorini, A., Grassi, D., Montabone, L., Lebonnois, S., Drossart, P., Piccioni, G., 2012. Investigation of air temperature on the nightside of Venus derived from VIRTIS-H onboard Venus-Express. Icarus 217, 640–647.

Mills, F.P., Esposito, L.W., Yung, Y.L., 2007. Atmospheric composition, chemistry, and clouds. In: Esposito, L.W., et al. (Eds.), Exploring Venus as a Terrestrial Planet, pp. 73–100.

Nevejans, D., et al., 2006. Compact high-resolution spaceborne echelle grating spectrometer with acousto-optical tunable filter based order sorting for the infrared domain from 2.2 to 4.3 μm. Appl. Opt. 45, 5191–5206. http://dx.doi.org/10.1364/AO.45.005191.

Niemann, H.B., Hartle, R.E., Hedin, A.E., Kasprzak, W.T., Spencer, N.W., Hunten, D.M., Carignan, G.R., 1979. Venus upper atmosphere neutral gas composition—first observations of the diurnal variations. Science 205, 54–56. http://dx.doi.org/10.1126/science.205.4401.54.

Niemann, H.B., Kasprzak, W.T., Hedin, A.E., Hunten, D.M., Spencer, N.W., 1980. Mass spectrometric measurements of the neutral gas composition of the thermosphere and exosphere of Venus. J. Geophys. Res. 85, 7817–7827. http://dx.doi.org/10.1029/JA085iA13p07817.

Parkinson, C.D., Gao, P., Schulte, R., Bougher, S.W., Yung, Y.-L., Bardeen, C.G., Wilquet, V., Vandaele, A.-C., Mahieux, A., Tellmann, S., Patzold, M., 2015. Distribution of sulfuric acid aerosols in the clouds and upper haze of Venus using Venus Express VAST and VeRA temperature profiles. Planet. Space Sci. 113-114, 205–219.

Piccialli, A., Montmessin, F., Bertaux, J.-L., Marcq, E., Fedorova, A., Korablev, O., Mahieux, A., Vandaele, A.-C., 2013. Density and Temperatures of Venus Upper Atmosphere Measured by Stellar Occultations with Spicav/Venus Express in European Planetary Science Congress 2013, 8–13 September, London, UK. Online at: ⟨http://meetings.copernicus.org/epsc2013⟩, id. EPSC2013-750, vol. 8, p. 750.

Rodgers, C.D., 2000. Inverse Methods for Atmospheric Sounding—Theory and Practice. In: Clive D. Rodgers (Ed.), Inverse Methods for Atmospheric Sounding—Theory and Practice. Series: Series on Atmospheric Oceanic and Planetary Physics, ISBN: ⟨ISBN⟩9789812813718⟨/ISBN⟩.World Scientific Publishing Co.Pte. Ltd., vol. 2. 2, doi: http://dx.doi.org/10.1142/9789812813718.

Roldán, C., López-Valverde, M.A., López-Puertas, M., Edwards, D.P., 2000. Non-LTE infrared emissions of CO_2 in the atmosphere of Venus. Icarus 147, 11–25. http://dx.doi.org/10.1006/icar.2000.6432.

Schubert, G., Bougher, S.W., Covey, A.D., Del Genio, C.C., Grossman, A.S., Hollingsworth, J.L., Limaye, S.S., Young, R.E., 2007. Venus atmosphere dynamics: a continuing enigma. In: Esposito, L.W., Stofan, E.R., Cravens, T.E. (Eds.), Exploring Venus as Terrestrial Planet, AGU Geophysical Monograph 176, pp. 121–138.

Seiff, A., Kirk, D.B., 1982. Structure of the Venus mesosphere and lower thermosphere from measurements during entry of the Pioneer Venus probes. Icarus 49, 49–70. http://dx.doi.org/10.1016/0019-1035(82)90056-2.

Sonnabend, G., Sornig, M., Krötz, P., Stupar, D., Schieder, R., 2008. Ultra high spectral resolution observations of planetary atmospheres using the Cologne tuneable heterodyne infrared spectrometer. J. Quant. Spectrosc. Radiat. Transf. 109, 1016–1029. http://dx.doi.org/10.1016/j.jqsrt.2007.12.003.

Sonnabend, G., Kroetz, P., Sornig, M., Stupar, D., 2010. Direct observations of Venus upper mesospheric temperatures from ground based spectroscopy of CO_2. Geophys. Res. Lett. 37, L11,102. http://dx.doi.org/10.1029/2010GL043335.

Soret, L., Gérard, J.-C., Montmessin, F., Piccioni, G., Drossart, P., Bertaux, J.-L., 2012. Atomic oxygen on the Venus nightside: global distribution deduced from

airglow mapping. Icarus 217 (2), 849–855. http://dx.doi.org/10.1016/j.icarus.2011.03.034.

Taylor, F.W., et al., 1980. Structure and meteorology of the middle atmosphere of Venus Infrared remote sensing from the Pioneer orbiter. J. Geophys. Res. 85, 7963–8006. http://dx.doi.org/10.1029/JA085iA13p07963.

Tellmann, S., Häusler, B., Hinson, D.P., Tyler, G.L., Andert, T.P., Bird, M.K., Imamura, T., Pätzold, M., Remus, S., 2012. Small-scale temperature fluctuations seen by the vera radio science experiment on Venus Express. Icarus 221 (2), 471–480.

Tellmann, S., Pätzold, M., Häusler, B., Bird, M.K., Tyler, G.L., 2009. Structure of the Venus neutral atmosphere as observed by the radio science experiment VeRa on Venus Express. J. Geophys. Res. (Planets) 114, E00B36. http://dx.doi.org/10.1029/2008JE003204.

Toon, O.B., Turco, R.P., Westphal, D., Malone, R., Liu, M.S., 1988. A multidimensional model for aerosols: description of computational analogs. J. Atmos. Sci. 45, 2123–2143.

Toon, O.B., Turco, R.P., Jordan, J., Goodman, J., Ferry, G., 1989. Physical processes in polar stratospheric ice clouds. J. Geophys. Res. 94, 11359–11380.

Turco, R.P., Hamill, P., Toon, O.B., Whitten, R.C., Kiang, C.S., 1979. A one-dimensional model describing aerosol formation and evolution in the stratosphere: I. Physical processes and mathematical analogs. J. Atmos. Sci. 36, 699–717.

Vandaele, A.-C., et al., 2013. Improved calibration of SOIR/Venus Express spectra. Opt. Express. 21, 21148–21161.

von Zahn, U., Fricke, K.H., Hoffmann, H., Pelka, K., 1979. Venus—eddy coefficients in the thermosphere and the inferred helium content of the lower atmosphere. Geophys. Res. Lett. 6, 337–340.

Wilquet, V., Drummond, R., Mahieux, A., Robert, S., Vandaele, A.-C., Bertaux, J.-L., 2012. Optical extinction due to aerosols in the upper haze of Venus: four years of SOIR/VEX observations from 2006 to 2010. Icarus 217, 875–881.

Zalucha, A.M., Brecht, A.S., Rafkin, S., Bougher, S.W., Alexander, M.J., 2013. Incorporation of a gravity wave momentum deposition parameterization into the venus thermosphere general circulation model (VTGCM). J. Geophys. Res. (Planets) 118 (1), 147–160. http://dx.doi.org/10.1029/2012JE004168.

Zhang, X., Liang, M.C., Mills, F.P., Belyaev, D., Yung, Y.-L., 2012. Sulphur chemistry in the middle atmosphere of Venus. Icarus 217, 714–739.